Highly magnetic Upper Miocene sandstones of the San Francisco Bay area, California

John W. Hillhouse and Robert C. Jachens,

U. S. Geological Survey, 345 Middlefield Road, MS 975, Menlo Park, California 94025, USA (jhillhouse@usgs.gov)

[1] A high-resolution aeromagnetic survey of the San Francisco Bay area shows prominent positive anomalies over distinctive blue sandstones of Late Miocene age. The total-field survey was measured at a nominal height of 300 m above the land surface along flight lines spaced 0.5 km apart. Anomalies with amplitudes up to 200 nT correlate with sandstones of the San Pablo Group, and these anomalies are similar in strength to the magnetic signatures of serpentinites and basalts in the surveyed region. Andesitic sandstone of the Neroly Formation, the upper part of the San Pablo Group, has high magnetic susceptibility (0.013 SI units, volume) and relatively strong natural remanent magnetization (0.29 A/m). Total magnetization of the sandstone is two thirds induced and one third remanent magnetization. The presence of coarse-grained magnetite detritus, low coercivity of remanence, low thermal stability of remanence, and multidomain properties is consistent with the NRM being a viscous remanent magnetization that grew during the Brunhes normal-polarity chron. The strong magnetic signature of the Upper Miocene sandstones allows their delineation over distances as great as 100 km, through areas where they are concealed by landslides and younger deposits. The sandstones are important structural markers for understanding the complex folding and faulting associated with active fault systems in the San Francisco Bay area.

1. Introduction

[2] An aeromagnetic survey of the San Francisco Bay region (Figures 1 and 2) reveals strongly positive magnetic anomalies over distinctive, widespread sedimentary beds. Rarely do sedimentary beds produce such a strong magnetic effect, which in this case is comparable in strength to the anomalies over igneous and metamorphic rocks of the region. The highly magnetic sedimentary beds are found within the San Pablo Group, which consists of the Cierbo Formation and the overlying Neroly Formation. The San Pablo Group is composed of sandstone and conglomerate of Late Miocene age. By combining detailed geologic mapping with the aeromagnetic survey, we can trace these distinctive beds over distances as great as 100 km beneath surficial deposits and across several active strands of the Calaveras and Hayward fault systems. The sandstones are important structural markers for efforts to understand the complex faulting and folding in the San Francisco Bay region during the past few million years [e.g., *McLaughlin et al.*, 1996].
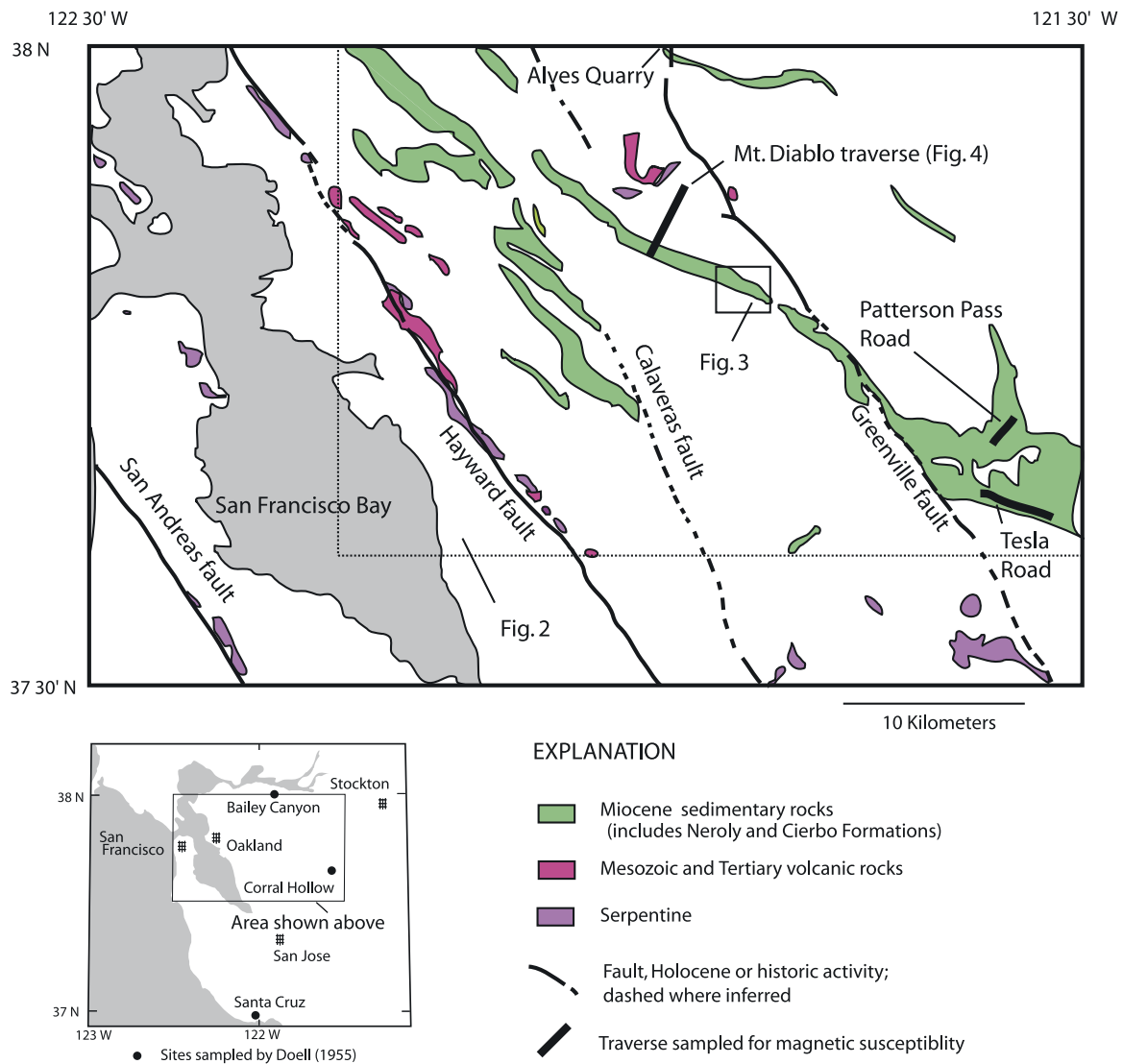
Geochemistry Geophysics Geosystems G³

Figure 1. Index location map of northern California, showing area of this study and sites (dots) investigated by *Doell* [1955]. Simplified geologic map of study area with strongly magnetic rock types highlighted. (Geology after *Wagner et al.* [1991]). Rock magnetic properties were measured at Alves Quarry, Mount Diablo, Patterson Pass Road, and Tesla Road.

[3] The primary objective of this study was to identify the source of strong magnetization in the San Pablo Group through characterization of its rock magnetic properties. Magnetic susceptibility and natural magnetic remanence were measured to assess the relative strength of remanent and induced magnetization. Also, coercivity of remanence, thermal stability, and strong-field magnetization were measured to assess iron-oxide mineralogy and magnetic grain sizes. Electron microprobe scans were made on polished grain mounts to chemically characterize the detrital grains and authigenic coatings. In addition to providing useful

data to aid in modeling subsurface structure, our study addresses a long-standing question concerning the role of diagenesis in the magnetization process.

[4] The first paleomagnetic study of the Neroly Formation by *Doell* [1955] revealed that strong natural remanent magnetization was acquired after the sandstone beds were folded. Doell proposed that the post-depositional magnetization was perhaps caused by chemical growth of magnetic minerals during diagenesis, and he coined the term "crystallization magnetization" to describe
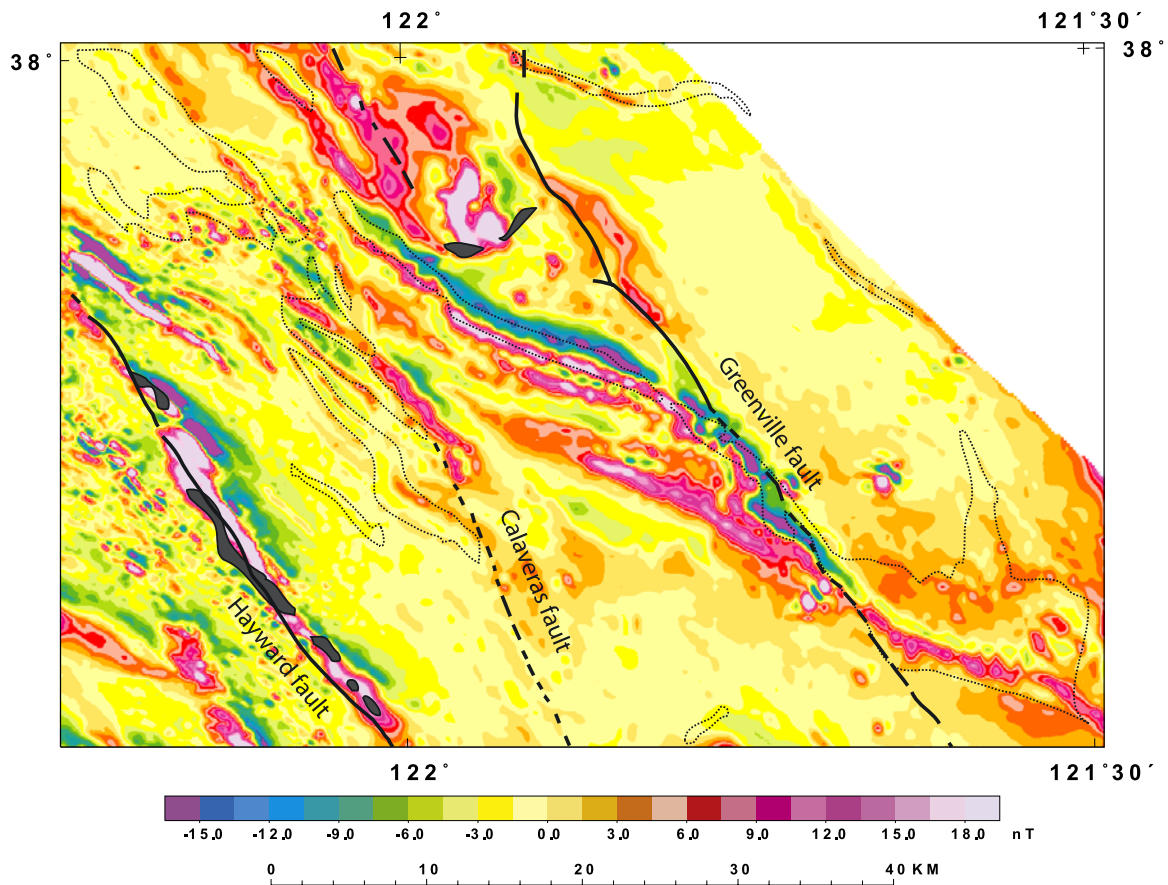
Figure 2. Map showing magnetic field measured in the study area shown in Figure 1. The magnetic data are presented in the form of the first vertical difference (100 m separation) of the total field data. This representation suppresses anomalies caused by deeply buried sources and emphasizes anomalies caused by rocks that lie very near the land surface or crop out. Mapped bodies of Neroly and Cierbo Formations are outlined in black dotted lines. Serpentinite and related ophiolitic rocks are shown in solid black. Many of the strong linear magnetic anomalies between the Calaveras and Greenville faults not associated with outcrops of Neroly or Cierbo Formations are inferred to be caused by these rocks concealed beneath younger deposits.

the process. Reporting paleomagnetic results from three widely separated sites (Figure 1, index map), Doell noted that all sandstone specimens had authigenic coatings around the detrital grains. He cited evidence that the coating was composed of iron-rich clay, implying mobilization of iron during diagenesis. The coating is white and translucent when viewed under magnification, although in combination with the generally dark detrital grains, the coating imparts a distinctive blue hue to the sandstone when viewed in hand samples. Doell proposed that secondary magnetic crystals, either on the detrital grain surfaces or in the pore space, might be the source of the natural remanent magnetization. Our second objective therefore was to investigate the origin of the post-depositional remanence in the Neroly Forma-

tion to see if diagenesis was the key to the relatively strong remanent magnetization of these blue sandstones.

2. Geologic and Geophysical Setting

[5] Our study involves an aeromagnetic survey, ground traverses, and collection of samples in Contra Costa and Alameda Counties east of San Francisco Bay (Figure 1). Geologically, the study area consists primarily of highly deformed and faulted clastic rocks and lesser occurrences of basalt, diabase, and serpentine [*Wagner et al.*, 1991; *Graymer et al.*, 1994]. The exposed basement rocks consist of two nearly coeval sequences, the Jura-Cretaceous Franciscan Complex in fault

contact with the Great Valley Sequence, including the Coast Range ophiolite. These rocks, which were juxtaposed in a convergent margin [*Ingersoll*, 1978], are overlain by a thick sequence of marine and non-marine sedimentary beds of Tertiary age and minor occurrences of Miocene and Pliocene volcanic rocks. Deposition of the younger sediments and volcanic rocks spanned the transition from a convergent tectonic regime to strike-slip motion along the Pacific-North American margin [*Nilsen and Clarke*, 1989]. Our study focuses on the Upper Miocene San Pablo Group, which includes the Neroly Formation in its upper part. The Neroly Formation, as described by *Huey* [1948], consists of sandstone and andesitic conglomerate (30 to 250 meters thick) beneath shales with minor coarser beds (up to 700 meters thick). The lower part contains the distinctive blue sandstones, which form prominent outcrops throughout the east-bay counties. Sandstones similar in age and lithology to the Neroly Formation are found in the Etchegoin Formation [*Dibblee*, 1973] to the south near Coalinga and in the Purisima Formation [*Clark et al.*, 1989] to the southwest near Santa Cruz (Figure 1). Both formations contain strongly magnetic sandstone beds.

[6] Lithologies of the blue sandstones are typically medium to coarse-grained, well-sorted, subangular grains of andesite similar in composition to the andesitic conglomerates. In the Tesla quadrangle, *Huey* [1948] described the sandstone as consisting largely of black microcrystalline to glassy lava particles in the light fraction; the heavy fraction, making up 13% of the sample, contained abundant augite with hornblende, hypersthene, and magnetite being commonly observed. Huey interpreted the depositional environment to be a broad coastal plain, largely nonmarine in the Tesla area, but becoming marine near Mount Diablo. The Neroly Formation coarsens to the east and can be traced in wells beneath the Great Valley. The Neroly Formation was presumed to be the distal facies of andesitic mudflows shed by volcanoes in the northern Sierra Nevada [*Louderback*, 1924], and recent investigations by *Walker* [2004] indicate northern Coast Range sources of sediment in addition to the Sierran provenance.

[7] The strong magnetization of the blue sandstones was noted in early magnetic surveys of the Etchegoin Formation in the Kettleman Hills oil field [*Lynton*, 1931]. *Brabb and Hanna* [1981] compiled aeromagnetic data for the southern San Francisco Bay region and called attention to the strong correlation between active fault zones, serpentinite, and magnetic gradients. Their maps show linear magnetic features now known to be associated with Miocene sedimentary beds, but the survey resolution was not sufficient to make a firm correlation of the linear features with the Neroly sandstone. Subsequent aeromagnetic studies in the San Francisco region, as summarized by *Jachens and Roberts* [1993], hinted that the Neroly Formation was a strong magnetic source, but the more recent high-resolution surveys [*U.S. Geological Survey*, 1992, 1996] (available at http://pubs.usgs.gov/of/2002/ofr-02-361/State_html/CA.htm; scroll down to data sets CA 4155 and CA 4167, respectively) show clearly the preponderance of positive magnetic anomalies above the sandstones (Figure 2). The newer total-field magnetic surveys were measured from fixed-wing aircraft at a nominal height of 300 m above the land surface along flight lines spaced 0.5 km apart. Total field magnetic data were measured with cesium precession magnetometers and positions were determined with Global Positioning System navigation equipment. The observed data were corrected for diurnal magnetic field variations, flight line data were adjusted relative to those of adjacent flight lines by the use of tie lines, and the International Geomagnetic Reference Field (updated to the dates of the surveys) was removed from the adjusted data. Detailed examination of the survey data reveal coherent, multiflight line total-field magnetic anomalies with amplitudes of a few nanoTesla (nT) or less, indicating that total measurement uncertainties are of this order or smaller.

[8] Anomaly amplitudes up to 200 nT correlate with the Neroly sandstones and the upper part of the Cierbo Formation. These anomalies are similar in strength to the magnetic signatures of serpentinites, diabases, and basalts in the surveyed region. Magnetic gradients measured above the sandstone beds are particularly prominent on the flanks of Mount Diablo, where the Tertiary strata are folded steeply into an anticline. (However, the strong magnetic anomalies directly over Mount Diablo are caused by pillow basalt and diabase in the axis of the anticline).

[9] The representative inset (Figure 3) near Tassajara shows the close correlation of linear magnetic features with the steeply dipping sedimentary beds of the San Pablo Group. In this
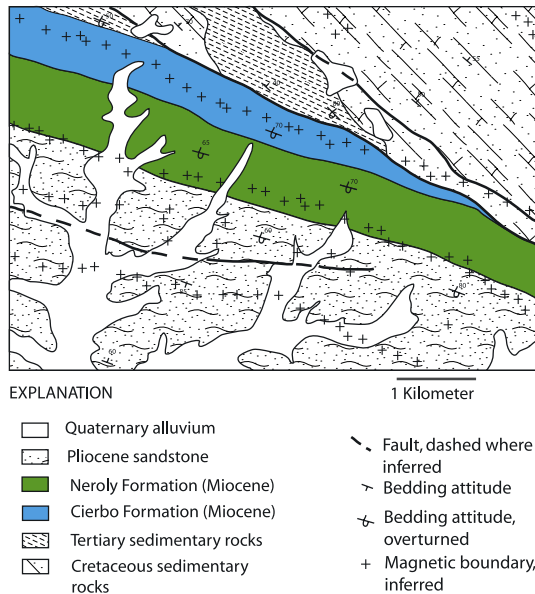
EXPLANATION

1 Kilometer

☐ Quaternary alluvium
▨ Pliocene sandstone
▨ Neroly Formation (Miocene)
▨ Cierbo Formation (Miocene)
▨ Tertiary sedimentary rocks
▨ Cretaceous sedimentary rocks

⟍ Fault, dashed where inferred
⊤ Bedding attitude
⊥ Bedding attitude, overturned
+ Magnetic boundary, inferred

Figure 3. Geologic map of area near Mt. Diablo (Figure 1) showing correlation of magnetic boundaries with Miocene sandstone formations.

example, the boundaries of magnetic bodies have been inferred from an automated procedure that converts the aeromagnetic data to pseudogravity, then solves for local maxima in the horizontal gradient of the resultant field [*Blakely and Simpson*, 1986]. Prominent magnetic boundaries follow the top of the Neroly Formation and the middle of the Cierbo Formation. Magnetic boundaries also align with upturned beds in the Pliocene sediments, which may be concealing underlying beds of the Neroly Formation.

[10] Close inspection of the more detailed aeromagnetic surveys beyond the area of Figure 1 shows other magnetic marker beds in sedimentary sections, particularly within Cretaceous strata of the Great Valley Sequence where one strongly magnetic bed extends for more than 150 km. *Lynton* [1931] described Cretaceous beds beneath the Etchegoin Formation near Coalinga as ''strongly magnetic,'' as well. Although we have limited our study to Miocene sedimentary rocks, the Cretaceous magnetic strata certainly warrant future work.

[11] To investigate the magnetic properties of the Neroly sandstone, we collected unoriented hand samples at four localities: Alves Quarry, Mount Diablo Road, Patterson Pass Road, and Tesla Road. The sites at Alves Quarry and Tesla Road are very close to two of *Doell*'s [1955] collection sites,

Bailey Canyon and Corral Hollow, respectively. We also conducted surveys of magnetic susceptibility with a hand-held meter along the three roadway sites, excluding Alves Quarry.

3. Magnetic Methods

[12] In making the road surveys, we measured susceptibility with a hand-held instrument by taking readings with the meter pressed against fresh sandstone exposed in roadcuts. As a check on the accuracy of this method, we also measured magnetic susceptibility with a Sapphire SI-2 system using specimens taken to the laboratory. The agreement of the two methods is within approximately 10%.

[13] Several tests involved measurement of magnetic remanence made with a superconducting magnetometer housed in a shielded room with the ambient magnetic field reduced to 500 nT. Specimens for the remanence and laboratory susceptibility measurements consisted of 10-cm³ cores cut from the hand samples. Isothermal remanence (IRM) curves were made by exposing each specimen to progressive direct fields up to 0.7 T in an electromagnet. The stability of remanence in both natural and IRM-treated specimens was tested by alternating-field demagnetization in a shielded reciprocating-tumbler in AC fields up to 100 mT. The unblocking-temperature distribution of natural remanence was measured in four specimens by heating them in air in a low-field (<5 nT) furnace, raising the temperature progressively to 600°C. For each temperature step, the specimen was heated and cooled during a 6-hour cycle, then measured in the magnetometer.

[14] An important clue to the chemical composition of magnetic minerals is the Curie point, the temperature above which ferromagnetic properties vanish. We inferred Curie temperatures from disaggregated specimens (approximately 50 milligrams), measuring magnetic susceptibility as the material was heated from room temperature to 700°C in argon. For these experiments, we used a Geophyzika CS-2 system at University of California, Santa Cruz.

[15] To draw inferences about the magnetic domain state of the magnetic minerals in these sandstones, we measured hysteresis loops and strong-field magnetization curves to derive coercivity of remanence, coercivity, saturation magnetization, and saturation remanent magnetization.
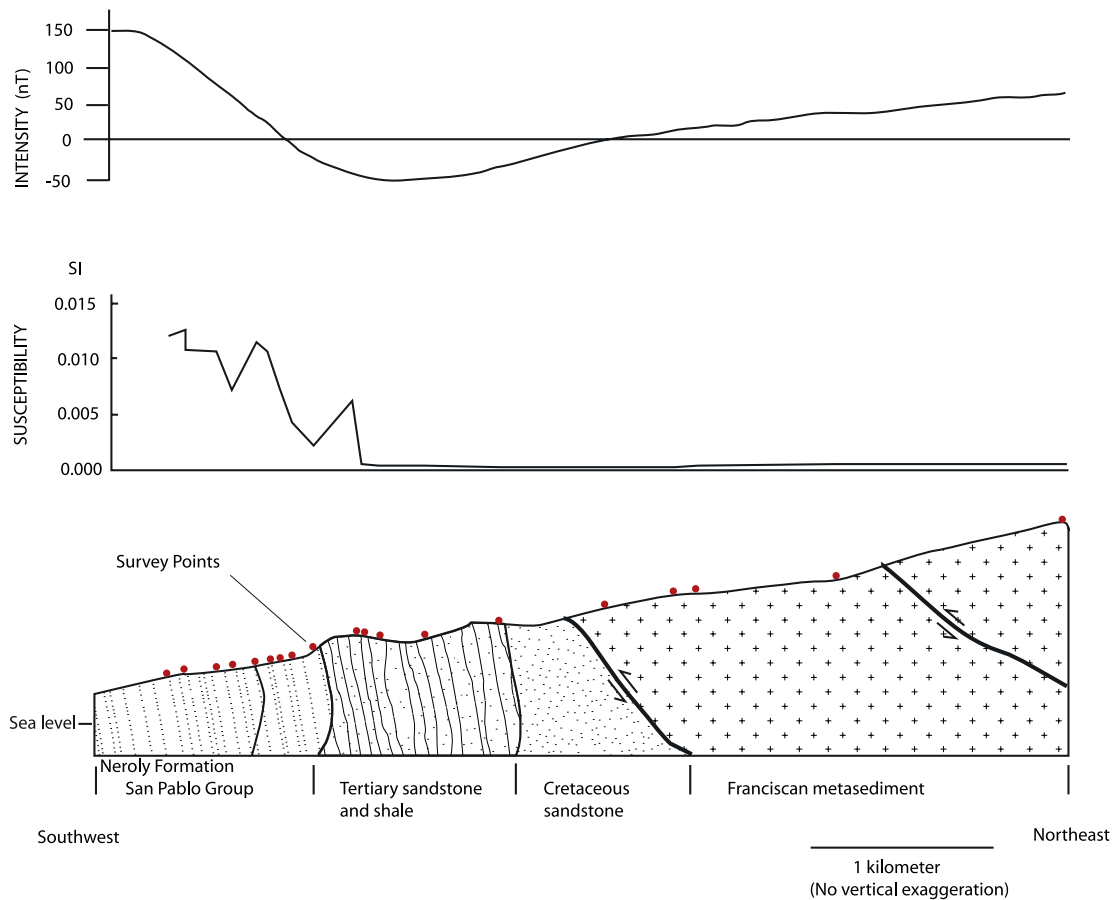
Figure 4. (top) Aeromagnetic anomaly, (middle) magnetic susceptibility survey, and (bottom) geologic cross section on west flank of Mount Diablo (Figure 1).

The device used for this purpose was a vibrating-sample magnetometer system at University of California, Santa Cruz. A small chip weighing a few milligrams was taken from each specimen core for this analysis.

4. Magnetic Results

[16] Our road surveys show the sharply higher magnetic susceptibility within the part of the San Pablo Group that includes the Neroly Formation and the upper half of the Cierbo Formation, in contrast to the values in the underlying sedimentary beds, particularly along Mount Diablo Road (Figure 4). The median value of susceptibility, derived from our road surveys and laboratory measurements, is 0.013 (SI per unit volume). This value is comparable to magnetic susceptibilities reported for nearby serpentinites and diabase [Mankinen et al., 1991], and is generally 100 times higher than other sedimentary formations in the region (Table 1). Stronger suscepti-

bility correlates with the blue sandy parts of the Neroly Formation.

[17] The magnetic perturbation of the sandstone per unit volume is given by the vector sum of induced and remanent magnetizations: $J_t = KH + J_r$, where J_t is the total magnetization vector, K is the bulk volume susceptibility, H is the ambient magnetic field vector, and J_r is the natural remanent magnetization vector. From the observations reported by Doell [1955], we know that the natural remanent magnetization of the Neroly sandstone is directed approximately parallel to the Earth's present magnetic field (declination: 16°; inclination: 61.5°). Therefore the induced and remanent magnetizations are parallel and the total magnetization of the sandstone can be treated as a simple scalar sum of the two. Our measurements of natural remanent magnetization and the strength of the Earth's magnetic field (40.58 A/m) indicate that the total magnetization vector of the sandstone averages 0.8 A/m

Table 1. Magnetic Properties of the Neroly Formation, San Francisco Bay Area[a]

Site	Latitude	Longitude	Sample Number	K	J_{nrm}	Q_n	Density
Alves Quarry	38.008	121.964	7J001-1	1.37	0.194	0.35	-
			7J001-2	1.49	0.213	0.35	1.72
			7J001-3	1.52	0.258	0.42	1.57
			7J001-4	1.61	0.235	0.36	1.66
			7J002-1	1.21	0.243	0.49	1.63
Mt. Diablo Road	37.843	121.947	7J003-1	1.80	0.386	0.53	2.22
			7J003-2	1.60	0.336	0.52	2.31
			7J003-3	1.81	0.378	0.51	2.44
	37.843	121.945	7J004-1	0.893	0.240	0.66	1.89
			7J004-2	0.923	0.243	0.65	2.12
	37.842	121.943	7J005-1	1.28	0.274	0.53	2.41
			7J005-2	1.14	0.233	0.50	2.20
	37.844	121.936	7J006-1	1.34	0.358	0.66	2.04
			7J006-2	1.28	0.337	0.65	2.23
Patterson Pass Road	37.691	121.593	8J001-1	1.49	0.331	0.55	1.38
			8J001-2	1.45	0.325	0.55	1.48
			8J001-3	1.43	0.366	0.63	1.55
			8J001-4	0.976	0.282	0.71	1.49
			8J001-5	1.26	0.346	0.68	1.50
			8J001-6	1.23	0.355	0.71	1.57
Tesla Road	37.649	121.601	8J003-1	0.990	0.262	0.65	1.57
			8J003-2	1.05	0.275	0.65	1.66
			8J003-3	1.06	0.276	0.64	1.64
			8J003-4	1.44	0.360	0.62	1.68
			8J003-5	1.29	0.326	0.62	1.65
			8J003-6	1.33	0.329	0.61	1.66
	37.648	121.608	8J005-1	1.68	0.278	0.41	1.66
			8J005-2	1.58	0.260	0.41	1.74
			8J005-3	1.42	0.238	0.41	1.67
			8J005-4	1.20	0.205	0.42	1.71
			8J005-5	1.69	0.255	0.37	1.73
			8J005-6	1.49	0.200	0.33	1.72
Mean				1.35	0.287	0.54	1.79

[a] Notes: K, volume magnetic susceptibility (10^{-2} SI units); J_{nrm}, natural remanent magnetization in A/m; Q_n, Koenigsberger ratio: $J_{nrm}/K\,H$, where H = 40.58 A/m (0.51 Oe); density in g/cm^3 with sample weighed dry.

(Table 1). The mean Koenigsberger value, or ratio of remanent to induced magnetization, ranges from 0.3 to 0.7 for the Neroly sandstone, having a median value of 0.5.

5. Properties of Rock Magnetism

[18] Rock magnetic experiments allow inferences to be made about the chemical composition, domain size, and concentration of magnetic minerals. These factors determine the overall magnetic response of any rock type. Tests of Curie temperature, unblocking temperature, and acquisition of isothermal remanence pertain to chemical composition and mineralogy of the magnetic grains. The hysteresis properties and other tests of coercivity are useful for determining effective magnetic do-main sizes. If the magnetic mineralogy is known, then saturation magnetization is a measure of concentration of the iron oxide.

[19] The susceptibility versus heating curves of two specimens from Alves Quarry give Curie temperatures of 540° to 580°C (Figure 5). Acquisition of isothermal remanence was tested on one specimen from Alves Quarry and two from Mount Diablo Road. The three curves are similar (Figure 6), showing near-saturation of IRM after applied fields of 0.15 T. Both Curie temperature and IRM responses are typical of rocks bearing titanomagnetite. The slight rise in IRM beyond 0.15 T indicates a small contribution from a high-coercivity iron oxide like hematite or limonite, but titanomagnetite is undoubtedly the primary constituent. Thermal demagnetizations of the natural
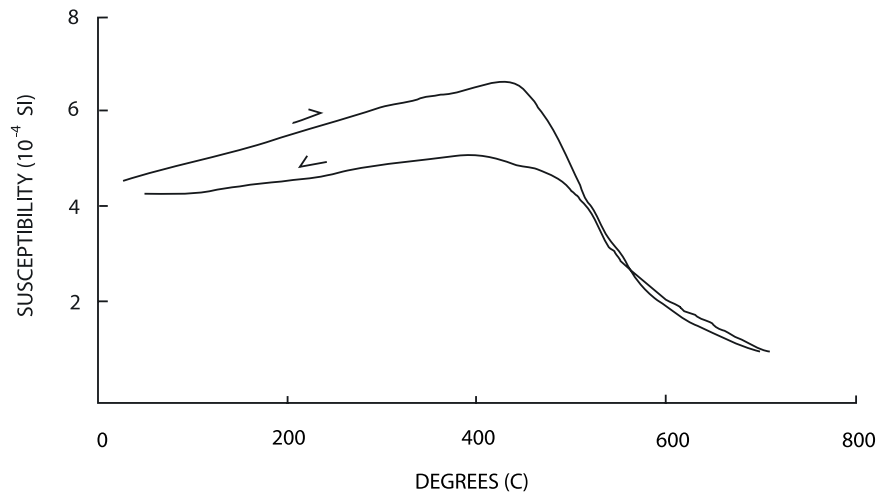
Figure 5. Response of magnetic susceptibility to heating a specimen of the Neroly sandstone from Alves Quarry.

remanence of one specimen from Patterson Pass Road and two from Tesla Road show that the magnetization is reduced to less than 3% of the initial value after heating to 556°C, also consistent with low-titanium titanomagnetite and no hematite being present.

[20] The response of NRM and IRM to alternating-field demagnetization was tested for a specimen from Alves Quarry and two from Mount Diablo Road (Figure 7). All three comparisons show the

NRM curve below the IRM curve, a response expected from multidomain or large-grained titanomagnetites [*Lowrie and Fuller*, 1971]. Results from this test are sometimes ambiguous, but the hysteresis curve of one specimen from Alves Quarry is supportive and definitive (Figure 8). Small separation of the forward and backward limbs is typical of multidomain behavior, and the ratios of H_{cr}/H_c (3.44) and M_{rs}/M_s (0.9) are consistent with the effective grain size being larger than single domain [*Day et al.*, 1977]. The Neroly
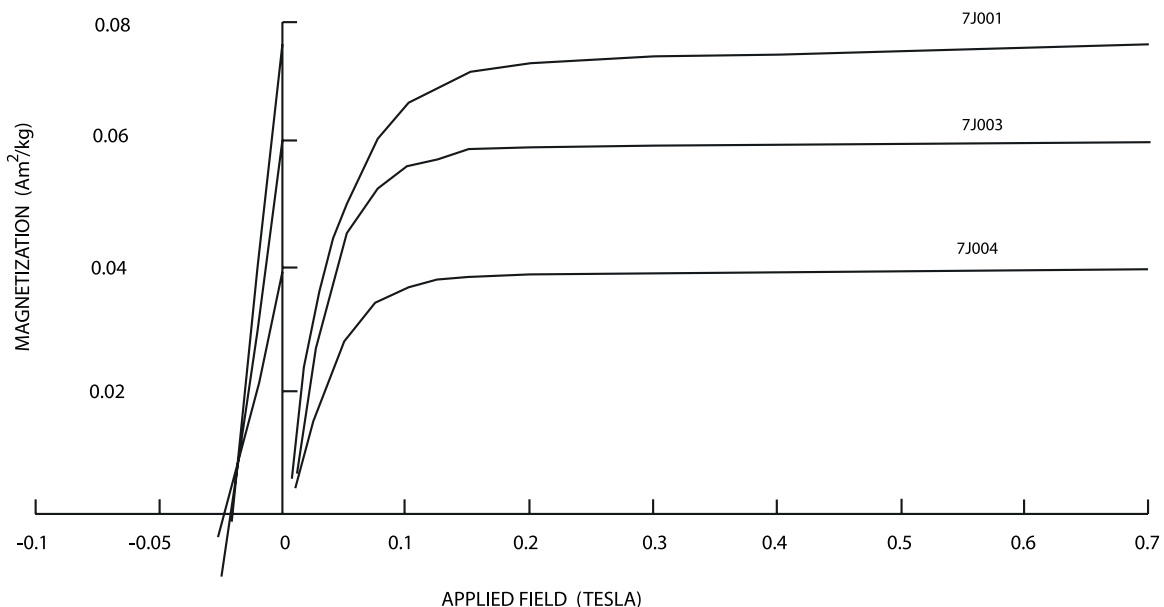

Figure 6. Acquisition of isothermal remanent magnetization of three specimens from the Neroly Formation. The back-field curves indicate coercivity or remanence of approximately 25 mT. See Table 1 for sample locations.
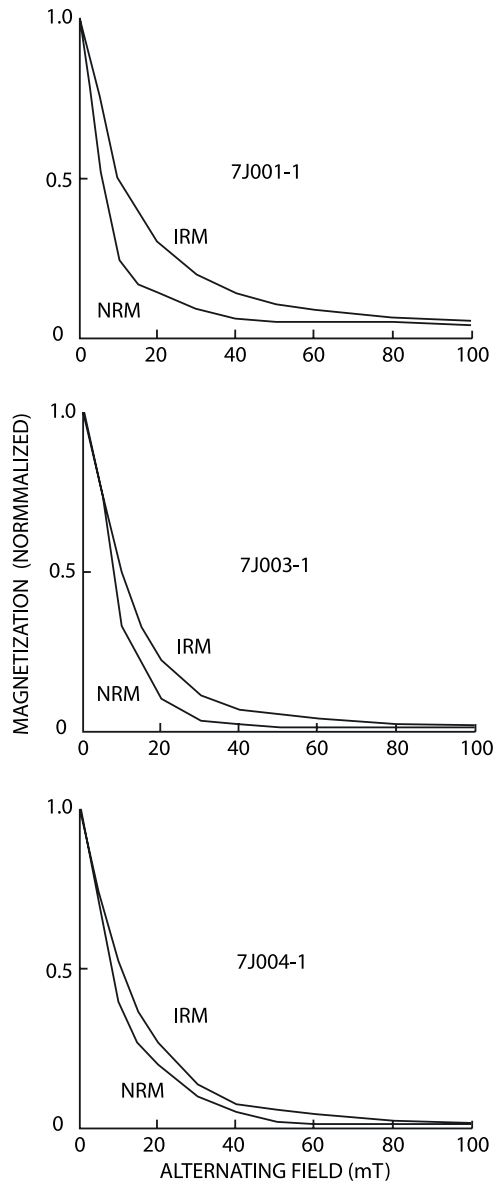
Figure 7. Comparison of responses of natural remanent magnetization (NRM) and isothermal remanent magnetization (IRM) to alternating-field demagnetization of Neroly sandstone. See Table 1 for sample locations.

sandstone probably contains a broad range of magnetic grain sizes. Nevertheless, a comparison of the rock-magnetic ratios from the Neroly with data from size-controlled fractions of magnetite is useful in characterizing the effective magnetic-grain size of the sandstone. Experimental data from crushed and sieved magnetites would suggest that the Neroly specimen has effective magnetic grain sizes of 1 to 10 micrometers [*Day et al.*, 1977; *Hartstra*, 1982]. Data from hydrothermally grown

magnetite grains, perhaps a better analog to naturally occurring minerals, suggest an effective grain size of 0.3–0.5 micrometers [*Heider et al.*, 1987; *Argyle and Dunlop*, 1990].

[21] In applied magnetic fields above 0.5 T, the Neroly specimen reached saturation and gave a magnetization value of 1.34 Am^2/kg. Given that pure magnetite has a saturation magnetization of 92 Am^2/kg, the mass concentration of iron oxide in this specimen is approximately 1.5%.

6. Electron Microprobe Analysis

[22] Iron oxides from the Alves Quarry specimen were concentrated with a hand-magnet, then the separate was prepared as a polished grain mount for electron microprobe analysis. For scanning, we selected an area of 400×400 micrometers on the polished surface containing seven lithic grains. The area was scanned at a resolution of 800×800 points with a beam energy of 15 kV (Figure 9). As shown in the backscattered-electron image, the grains are phenocrystic and each is coated. The grains are 50 to 150 micrometers in diameter, and the coatings are approximately 15 micrometers thick. The test area was scanned for five elements: magnesium, iron, silicon, titanium, and aluminum. The brightest areas within each grain, as shown in the backscattered image, are titanomagnetite. Titanium is limited to these crystals and has an abundance of 10% to 15% relative to iron. Close inspection of the iron and titanium scans indicates fine structure due to ilmenite lamellae within the titanomagnetite crystals. This partitioning of the two minerals is the product of deuteric alteration, commonly observed in extrusive volcanic rocks. Scanning of the remaining phenocrysts and matrix, plus spot analyses, indicated that the lithic grains in addition to titanomagnetite contain augite, hypersthene, hornblende, and glass typical of andesite.

[23] The diagenetic coating on each grain is an iron-aluminum silicate. Five spot analyses (10 micrometer beam size) of the coating gave an average composition of 67% silica, 14% alumina, 10% ferrous oxide, 5% magnesium oxide, and 2% calcium oxide. The other analyzed elements (sodium, potassium, titanium, and manganese) had concentrations of less than 1%. *Doell* [1955] cited evidence that the grain-coatings in the Neroly sandstone were iron-rich clays with montmorillonite structure, not inconsistent with our chemical analysis of the material. Doell also noted that although the coating itself was not ferromagnetic, it enclosed
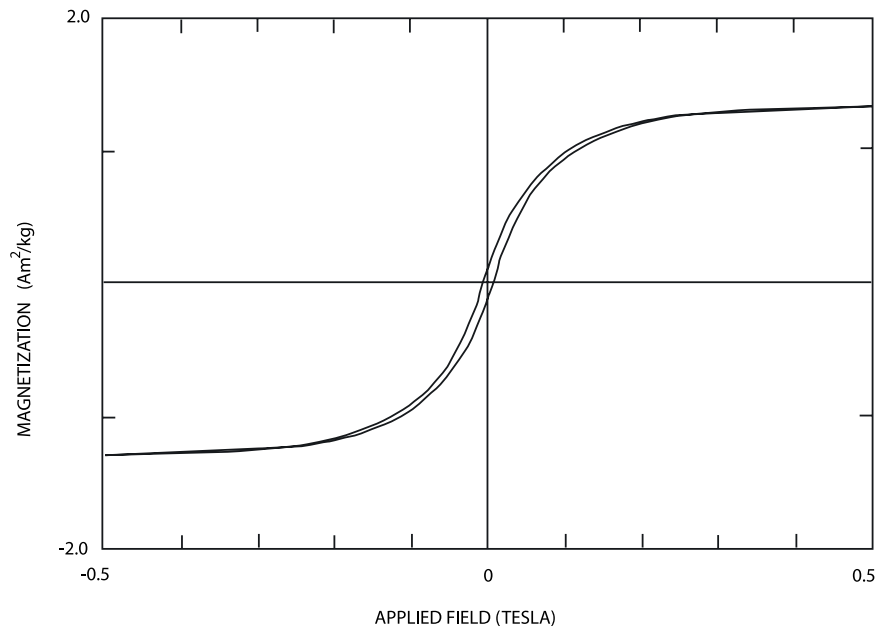
Figure 8. Hysteresis curve of magnetization versus applied field for a specimen of Neroly sandstone from Alves Quarry.

iron-oxide microcrystals of authigenic origin. Our electron-probe analysis did not confirm the presence of such microcrystals, but later microscopic examination showed very thin rims of a possibly opaque mineral at the outer margins of some coated grains. If the rims contain iron oxide, then the mineral is probably hematite or limonite produced by low-temperature oxidation. Our rock magnetic tests (thermal demagnetization and IRM acquisition) of the Neroly specimens showed that
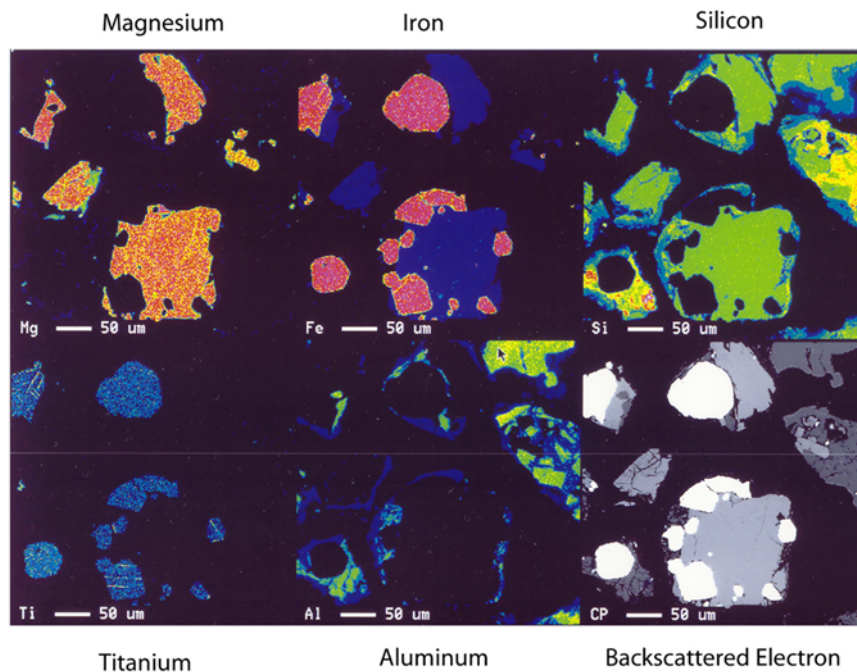

Figure 9. Electron-probe scans of a polished grain mount: Neroly sandstone from Alves Quarry. White areas in backscattered-electron image are titanomagnetite crystals. In the silicon scan, blue areas on the grain margins are the clay-like authigenic coating.

hematite or related secondary iron-oxides contribute very little to the magnetic behavior of the sandstone.

7. Discussion

[24] From all evidence gathered, we find that the Neroly sandstone contains a relatively large concentration of coarse-grained titanomagnetite of detrital origin. The magnetic response of the sediment to applied fields and heating is very "soft", meaning that the magnetic-domain structure is readily changed by ambient magnetic fields and thermal perturbations. Induced magnetization is the dominant part of the total magnetization of the sandstone, accounting for two thirds of the positive aeromagnetic anomaly. Susceptibility is proportional to the concentration of the magnetic grains, so we would expect strong susceptibility given the large concentration of titanomagnetite observed. In addition, susceptibility per unit volume rises with increasing grain size, reaching the maximum value in multidomain magnetite when the grain diameter exceeds approximately 10 micrometers [Day et al., 1977; Hartstra, 1982]. This grain-size effect, believed due to easy movement of domain walls in the applied field, contributes to the strong susceptibility of the Neroly sandstone.

[25] One third of the anomaly produced by the Neroly sandstone can be traced to its natural remanence. Doell's [1955] work with oriented samples from the same region as our study showed that natural remanent magnetization was acquired after the beds had been tilted to dips ranging from 8° to 90°. Not correcting for tilt, the natural remanent magnetization is nearly parallel to the normal-polarity axial dipole field and hence essentially parallel to the induced magnetization.

[26] After deposition, all rocks begin to acquire viscous remanent magnetization (VRM), whereby thermal fluctuations and the Earth's field slowly change the material's magnetization toward the ambient field direction. With its soft magnetic properties, the Neroly sandstone would be particularly vulnerable to acquiring VRM. In the laboratory, thermal demagnetization from 200° to 300°C will usually remove VRM [Wilson and Smith, 1968; Dunlop, 1969] acquired by magnetite during the most recent polarity epoch. The natural remanent magnetization of the Neroly sandstone, however, is 90% removed after heating to 330°C,

and an underlying component is not found. Therefore we suspect that VRM is nearly the entire natural remanent magnetization.

[27] In a steady ambient magnetic field, VRM grows at a rate proportional to the logarithm of the exposure time [Dunlop, 1973]. From structural observations, we can estimate the amount of time that the folded Neroly strata were exposed to the Earth's normal-polarity dipole field. In the region, gravels of early Pleistocene age are tilted, so the Neroly natural remanent magnetization must be younger than 1.6 Ma. If tilting of the Neroly Formation has been minor since the middle Pleistocene, as implied by minor folding in nearby younger deposits, then we can assume that the body of sediment has remained stationary relative to the Earth's normal-polarity field throughout the Brunhes Normal Chron. The exposure time is therefore 780,000 years [Cande and Kent, 1995].

[28] The VRM growth rate is also proportional to the temperature of the material during exposure to the ambient field. According to Burke et al. [1997], fission track data indicate burial temperatures of 55° to 70°C before uplift of the core of the Mount Diablo anticlinorium. Their measurements are from Franciscan rocks on the peak of Mount Diablo, hence the resultant temperature range would be the maximum heating expected for the folded Neroly Formation on the outer flanks of the anticlinorium.

[29] Theoretical calculations of VRM acquisition permit prediction of laboratory-derived unblocking temperatures from the estimated time-temperature conditions of natural exposure [Dunlop, 1977; Pullaiah et al., 1975]. For single-domain magnetite under the conditions noted above for the Neroly sandstone, the expected maximum unblocking temperature measured in the laboratory would be 250°C if the magnetization is entirely VRM. Because the Neroly sandstone exhibits multidomain properties, viscosity calculations based on single-domain theory might not be applicable here. However, experimental determinations of VRM acquisition in magnetite grains indicate nearly constant acquisition coefficients for grain diameters from 0.2 to 45 micrometers, which includes the estimated effective grain sizes of the Neroly sandstone [Tivey and Johnson, 1984]. As shown in Figure 10, 80% of the natural remanence of the specimen from the Neroly Formation at Mount Diablo is unblocked by heating up to 250°C. Experiments with some
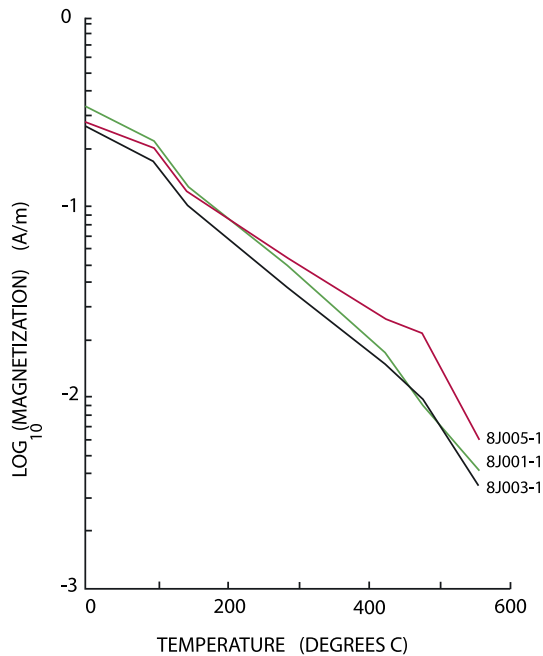
Figure 10. Thermal demagnetization results from specimens of the Neroly sandstone. See Table 1 for sample locations.

natural materials have differed from predictions from VRM theory, in that VRM has shown unexpectedly high resistance to thermal demagnetization. Although not all of the Neroly natural remanence can be accounted for by VRM theory, a completely viscous origin of the magnetization

is permissible in view of uncertainties in the theory as applied to this natural material.

[30] We conducted a ten-day shelf test on eight specimens to determine the short-term magnetic viscosity of the sandstone at room temperature (Figure 11). The shelf test consisted of placing the specimens on a rack oriented so that the laboratory ambient magnetic field (42 A/m) was aligned parallel to the cylindrical axis of each specimen. Measurements of the remanent magnetization were taken five times during the ten-day period by removing the specimens from the rack for several minutes to be placed in the low-field chamber of the magnetometer. The viscosity coefficient, S_a, is given by the well-known relation: $J_t - J_o = S_a \log(t)$, where J_t is the magnetization after time t, and J_o is the initial magnetization. The shelf test was conducted for companion specimens, one held in the natural state and the other starting from the demagnetized state (100 mT). The resultant values of S_a for the ten-day acquisition period range from 0.01 to 0.03 A/m; the higher values are from specimens that were demagnetized at the beginning of the test. Extrapolating the VRM acquisition time to 780,000 years, or 8.5 orders of magnitude beyond the experiment duration, gives magnetizations (0.09 to 0.26 A/m) similar to the observed natural remanent magnetizations of the Neroly sandstone (Table 1). Again, ascribing the total natural remanence to VRM is permissible given our results from the shelf test,
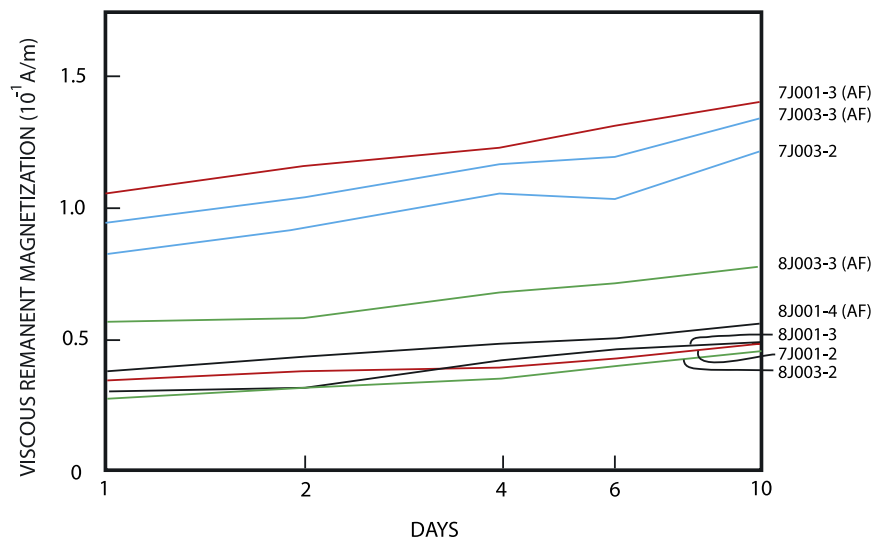

Figure 11. Acquisition of viscous remanent magnetization in the Neroly sandstone. Labels with (AF) indicate specimens initially demagnetized in alternating fields to 100 mT. Other specimens underwent no demagnetization treatments. See Table 1 for sample locations.

although we cannot be sure that the short-term acquisition coefficients accurately reflect long-term values.

[31] What effect, if any, did diagenesis have on the magnetic properties of the Neroly sandstone? Petrographic examination shows that the sandstone is well-sorted and loosely packed, implying high permeability. The hypersthene grains show etching due to intrastratal dissolution which led to precipitation of clay-like coatings on all of the detrital grains [*Williams et al.*, 1954, p. 309]. The solution effects are primarily confined to grain surfaces, as most of the lithic grains retain pristine cores. Although some iron was mobilized in this authigenic process, it mostly combined with aluminum to form a non-magnetic clay mineral. We found no evidence that appreciable amounts of iron-oxide, except very faint rims of hematite or limonite, formed during diagenesis. Our data suggest that the strong susceptibility and natural remanence of the Neroly sandstone arise from large-grained magnetite of detrital origin, and that diagenesis was not a major influence on the magnetic properties.

[32] Recognition of the Miocene sedimentary rocks as important sources of aeromagnetic anomalies opens the door for improved models of the subsurface structure of the San Francisco Bay area. Thickness and structure of the Miocene beds are now quite well known from several decades of geologic mapping, which provides control for three-dimensional modeling. Such control for aeromagnetic modeling may be lacking or be less certain for serpentinites and igneous intrusive rocks, which often have unpredictable contacts below the surface. It is beyond the scope of this paper to present detailed structural models of the region. However, an example that illustrates the usefulness of the magnetic marker beds involves determination of the northern end of the active Calaveras fault (Figure 1). Trenching shows that the northern Calaveras fault has a Holocene slip rate of 5 ± 2 mm/yr [*Kelson et al.*, 1996]. The fault poses a significant earthquake hazard for Bay Area residents (an 18% probability of a magnitude 6.7 or greater earthquake by 2030, according the U.S. Geological Survey estimates). Due to poor exposure of the fault trace in San Ramon Valley, it is not known whether the fault continues northward on the same trend or the slip is transferred to structures on either side of the main trace. A magnetic lineament above Neroly sandstone extends without deviation into an area covered by alluvium where the Calaveras fault has been inferred. Hence, the Calaveras fault must end before reaching the lineament, and its slip is accommodated by stepping west into a series of faults and folds [*Wakabayashi and Sawyer*, 1999; *Unruh et al.*, 2002; *Jachens et al.*, 2002; *Walker and Graymer*, 2003].

8. Conclusions

[33] High-resolution magnetic surveys of the San Francisco Bay region revealed that the Upper Miocene San Pablo Group, which includes a distinctive andesitic sandstone unit in the Neroly Formation, produces strong magnetic anomalies. Two thirds of the Neroly anomaly is induced magnetization caused by abundant titanomagnetite of detrital origin. The relatively high concentration of iron oxide is probably the combined effect of the volcanic source material, which tends to be rich in titanomagnetite, and the depositional process. The strongly magnetic part of the Neroly Formation consists of well-sorted, medium to coarse-grained sand that was deposited on a coastal floodplain. Clay and silt were winnowed out during deposition, leaving a heavy-mineral concentrate.

[34] Apparently, any magnetic remanence that the sediment acquired during deposition has been replaced by viscous remanent magnetization after the Neroly Formation was folded. The remanent magnetization approximately parallels the present geomagnetic field and accounts for one third of the aeromagnetic signal. The Miocene sandstone may have failed to develop appreciable depositional remanence from the beginning, because the detrital grains were too large to become aligned by the weak force of the ambient geomagnetic field. More importantly, the sandstone has "soft" magnetic properties that would lower time-stability of remanence while enhancing the growth of viscous magnetization. Rock magnetic tests (coercivity of remanence, ratio of saturation remanence to saturation magnetization, unblocking temperature distribution) indicate that the Neroly sandstone has effective magnetic grain sizes in the multidomain range. "Soft" magnetic properties of multidomain magnetite, thought to be a manifestation of easy movement of domain walls in response to energy perturbations, contribute to the high susceptibility and magnetic viscosity of the Neroly sandstone. Given the

availability of high-resolution aeromagnetic data, these strongly magnetic sedimentary beds are useful for modeling three-dimensional structure and delineating active faults in the San Francisco Bay region.

Acknowledgments

References

Argyle, K. S., and D. J. Dunlop (1990), Low-temperature and high-temperature hysteresis of small multidomain magnetites (215–540 nm), *J. Geophys. Res.*, *95*, 7069–7083.

Blakely, R. J., and R. W. Simpson (1986), Approximating edges of source bodies from magnetic or gravity anomalies, *Geophysics*, *51*, 1494–1498.

Brabb, E. E., and W. F. Hanna (1981), Maps showing aeromagnetic anomalies, faults, earthquake epicenters, and igneous rocks in the southern San Francisco Bay region, California, *U.S. Geol. Surv. Geophys. Invest. Map*, *GP-932*, scale 1:125,000.

Burke, J., R. Burgmann, and T. Dimitru (1997), Uplift of Mount Diablo using apatite fission tracks and geomorphic analysis (abstract), *Eos Trans. AGU*, *78*(46), Fall Meet. Suppl., F631.

Cande, S. C., and D. V. Kent (1995), Revised calibration of the geomagnetic polarity timescale for the Late Cretaceous and Cenozoic, *J. Geophys. Res.*, *100*, 6093–6095.

Clark, J. C., E. E. Brabb, and R. J. McLaughlin (1989), Geologic map and structure sections of the Laurel 7.5′ quadrangle, Santa Clara and Santa Cruz Counties, California, *U.S. Geol. Surv. Open File Rep.*, *89-676*, scale 1:24,000.

Day, R., M. Fuller, and V. A. Schmidt (1977), Hysteresis properties of titanomagnetites: Grain size and compositional dependence, *Phys. Earth Planet. Inter.*, *13*, 260–267.

Dibblee, T. W., Jr. (1973), Stratigraphy of the southern Coast Ranges near the San Andreas fault from Cholame to Maricopa, California, *U.S. Geol. Surv. Prof. Pap.*, *764*, 45 pp.

Doell, R. R. (1955), Remanent magnetization of the Upper-Miocene 'blue' sandstones of California, *J. Geophys. Res.*, *37*, 156–167.

Dunlop, D. J. (1969), Comments on a paper by R. L. Wilson and Peter J. Smith, "The nature of secondary natural magnetizations in some igneous and baked rocks", *J. Geomagn. Geoelectr.*, *21*, 797–801.

Dunlop, D. J. (1973), Theory of the magnetic viscosity of lunar and terrestrial rocks, *Rev. Geophys.*, *11*, 855–901.

Dunlop, D. J. (1977), Rocks as high-fidelity tape recorders, *IEEE Trans. Magn.*, *MAG-13*, 1267–1271.

Graymer, R. W., D. L. Jones, and E. E. Brabb (1994), Preliminary geologic map emphasizing bedrock formations in Contra Costa County, California, *U.S. Geol. Surv. Open File Rep.*, *94-622*, scale 1:75,000.

Hartstra, R. L. (1982), Grain-size dependence of initial susceptibility and saturation magnetization-related parameters of four natural magnetites in the PSD-MD range, *Geophys. J. R. Astron. Soc.*, *71*, 477–495.

Heider, F., D. J. Dunlop, and N. Sugiura (1987), Magnetic properties of hydrothermally recrystallized magnetite crystals, *Science*, *236*, 1287–1290.

Huey, A. S. (1948), Geology of the Tesla Quadrangle, California, *Bull. Calif. Div. Mines Geol.*, *140*, 75 pp.

Ingersoll, R. V. (1978), Paleogeography and paleotectonics of the late Mesozoic forearc basin of northern and central California, in *Mesozoic Paleogeography of the Western United States: Pacific Coast Paleogeography Symposium 2, Pacific Section*, edited by D. G. Howell and K. A. McDougall, pp. 471–482, Soc. of Econ. Paleontol. and Mineral., Tulsa, Okla.

Jachens, R. C., and C. W. Roberts (1993), Aeromagnetic map of the San Francisco Bay Area, California, *U.S. Geol. Surv. Geophys. Invest. Map*, *GP-1007*, scale 1:286,500.

Jachens, R. C., C. M. Wentworth, R. W. Graymer, J. P. Walker, F. C. Chuang, R. W. Simpson, and R. J. McLaughlin (2002), The Calaveras fault, northern California: A geophysical perspective on offset and 3-D geometry, *Eos Trans. AGU*, *83*(47), Fall Meet. Suppl., Abstract T71E-1205.

Kelson, K. I., G. D. Simpson, W. R. Lettis, and C. C. Haraden (1996), Holocene slip rate and earthquake recurrence of the northern Calaveras fault at Leyden Creek, northern California, *J. Geophys. Res.*, *101*, 5961–5975.

Louderback, G. D. (1924), Period of scarp production in the Great Basin, *Univ. Calif. Publ. Geol. Sci.*, *15*, 1–44.

Lowrie, W., and M. Fuller (1971), On the alternating field demagnetization characteristics of multidomain thermoremanent magnetization in magnetite, *J. Geophys. Res.*, *76*, 6339–6349.

Lynton, E. D. (1931), Some results of magnetometer surveys in California, *Am. Assoc. Pet. Geol. Bull.*, *15*, 1351–1370.

Mankinen, E. A., C. S. Gromme, and K. M. Williams (1991), Concordant paleolatitudes from ophiolite sequences in the northern California Coast Ranges, U.S.A., *Tectonophysics*, *198*, 1–21.

McLaughlin, R. J., W. V. Sliter, D. H. Sorg, P. C. Russell, and A. M. Sarna-Wojcicki (1996), Large-scale right-slip displacement on the East San Francisco Bay Region fault system, California: Implications for location of late Miocene to Pliocene Pacific plate boundary, *Tectonics*, *15*, 1–18.

Nilsen, T. H., and S. H. Clarke, Jr. (1989), Late Cenozoic basins of northern California, *Tectonics*, *8*, 1137–1158.

Pullaiah, G., E. Irving, K. L. Buchan, and D. J. Dunlop (1975), Magnetization changes caused by burial and uplift, *Earth Planet. Sci Lett.*, *28*, 133–143.

Tivey, M., and H. P. Johnson (1984), The characterization of viscous remanent magnetization in large and small magnetite particles, *J. Geophys. Res.*, *89*, 543–552.

U.S. Geological Survey (1992), Aeromagnetic map of Livermore and vicinity, California, *U.S. Geol. Surv. Open File Rep.*, *92-531*, scale 1:250,000.

U.S. Geological Survey (1996), Aeromagnetic map of the central San Francisco Bay area, California, *U.S. Geol. Surv. Open File Rep.*, *96-530*, scale 1:100,000.

Unruh, J. R., K. I. Kelson, D. Manaker, and A. Barron (2002), Critical evaluation of the northern termination of the Calaveras fault, San Francisco Bay area, final technical report, 72 pp., U.S. Geol. Surv., Menlo Park, Calif.

Wagner, D. L., E. J. Bortugno, and R. D. McJunkin (1991), Geologic map of the San Francisco-San Jose quadrangle, *Regional Geol. Map Ser.*, *Map 5A*, scale 1:250,000, Calif. Div. of Mines and Geol., Sacramento.

Wakabayashi, J., and T. L. Sawyer (1999), Slip transfer from the northern Calaveras fault: A critical unresolved seismic hazard issue in the eastern San Francisco Bay region, *Eos Trans. AGU*, *80*(46), Fall Meet. Suppl., F735.

Walker, J. P. (2004), Provenance of Tertiary conglomerates, eastern San Francisco Bay area, California, M.S. thesis, 97 pp., Calif. State Univ., San Jose.

Walker, J. P., and R. W. Graymer (2003), Absence of late Neogene offset on the northern Calaveras fault, *Eos Trans. AGU*, *84*(46), Fall Meet. Suppl., Abstract T12E-07.

Williams, H., F. J. Turner, and C. M. Gilbert (1954), *Petrography*, 406 pp., W. H. Freeman, New York.

Wilson, R. L., and P. J. Smith (1968), The nature of secondary natural magnetizations in some igneous and baked rocks, *J. Geomagn. Geoelectr.*, *20*, 367–380.